Progress in Natural Science: Materials International 2012;22(5):452–460

Chinese Materials Research Society

Progress in Natural Science: Materials International

www.elsevier.com/locate/pnsmi
www.sciencedirect.com

ORIGINAL RESEARCH

Designing of ECAP parameters based on strain distribution uniformity

F. Djavanroodi, B. Omranpour, M. Ebrahimi*, M. Sedighi

Department of Mechanical Engineering, Iran University of Science and Technology, Tehran, Iran

Received 21 May 2012; accepted 5 August 2012
Available online 30 October 2012

KEYWORDS

ECAP;
FEM;
Die design;
Strain distribution

Abstract Equal Channel Angular Pressing (ECAP) is currently one of the most popular methods for fabricating Ultra-Fine Grained (UFG) materials. In this work, ECAP process has been performed on commercial pure aluminum up to 8 passes by route *A*. After verification of FEM work, the influences of four die channel angles, three outer corner angles and pass number up to 8 have been analyzed to investigate strain distribution behavior of ECAPed material. Two methods for quantifying the strain homogeneity namely inhomogeneity index (C_i) and standard deviation (S.D.) are compared. It is shown that C_i is not a good candidate for examining the strain distribution uniformity. Moreover, it is suggested that designing of ECAP die geometry to achieve optimum strain distribution homogeneity is more suitable than the optimum effective strain magnitude. The best strain distribution uniformity in the transverse plane is obtained with $\Phi = 60^\circ$ and $\Psi = 15^\circ$ and for the bulk of the sample, $\Phi = 120^\circ$ and $\Psi = 15^\circ$ or 60°, gives the highest strain dispersal uniformity.

1. Introduction

Equal Channel Angular Pressing developed by Segal [1] is the most popular Severe Plastic Deformation (SPD) techniques for enhancement of mechanical properties and superplastic behavior with respect to the grain size reduction [2–4]. As a principle, material grain size is one of the prominent parameters influencing mechanical behavior of base metals and alloys concentrated in all of the SPD techniques like ECAP [5], High Pressure Torsion (HPT) [6], Accumulative Roll Bonding (ARB) [7], Constrained Groove Pressing (CGP) [8], Accumulative Back Extrusion (ABE) [9], Tubular Channel Angular

*Corresponding author. Tel.: +98 217 724 0203.
E-mail addresses: javanroodi@iust.ac.ir (F. Djavanroodi), omranpour@yahoo.com (B. Omranpour), mebrahimi@iust.ac.ir (M. Ebrahimi), sedighi@iust.ac.ir (M. Sedighi).

Peer review under responsibility of Chinese Materials Research Society.

ELSEVIER Production and hosting by Elsevier

http://dx.doi.org/10.1016/j.pnsc.2012.08.001

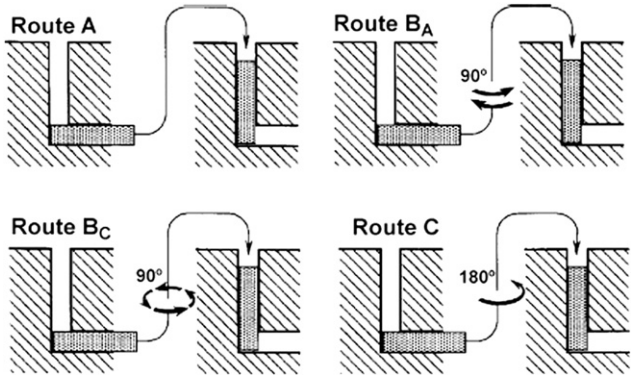

Fig. 1 Four fundamental routes in the ECAP process [12].

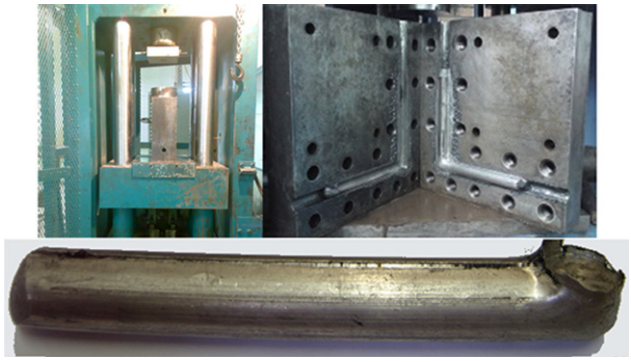

Fig. 2 Hydraulic press, ECAP die and AL billet after one pass pressing.

Pressing (TCAP) [10], etc. During ECAP, a sample is pressed through two intersecting channels having the same cross-sections with a die channel angle of Φ and an outer corner angle of Ψ. During this process, billet with high value of plastic strain can be produced because of accumulative shear strain at each pass. The magnitude of shear strain after one pass ECAP in the frictionless condition is determined with [11]:

$$\gamma = 2cot\left(\frac{\Phi+\Psi}{2}\right) + \Psi cosec\left(\frac{\Phi+\Psi}{2}\right) \quad (1)$$

Also, the magnitude of equivalent effective plastic strain (ε_{eq}) after N passes is given by the following relationship:

$$\varepsilon_{eq} = N/\sqrt{3}\left[2cot\left(\frac{\Phi+\Psi}{2}\right) + \Psi cosec\left(\frac{\Phi+\Psi}{2}\right)\right] \quad (2)$$

In the ECAP process, there are four fundamental routes between each repetitive pressing as shown in Fig. 1 [12]. These are as follows: route A by which the sample is repetitively pressed without any rotation, route B_A by which the sample is rotated by 90° in the alternative direction between each pass, route B_C by which the sample is rotated in the same direction by 90° and route C by which the sample is rotated by 180° between consecutive passes. These routes result in different slip systems in the specimen and so, various microstructures and mechanical properties can be obtained by them [12,13].

So far, many experimental studies have been performed to investigate the influence of different pressing routes on the microstructure, texture and so, mechanical properties of the final work-piece [14,15]. Investigations of Komura et al. [16]

Table 1 Mechanical properties of pure Al before and after ECAP process up to 8 passes by route A.

No. of passes	Pass 0	Pass 1	Pass 2	Pass 3	Pass 4	Pass 8
YS (MPa)	39	87	118	136	145	153
UTS (MPa)	83	144	165	178	186	192
EL (%)	36	19	15	14	14	12

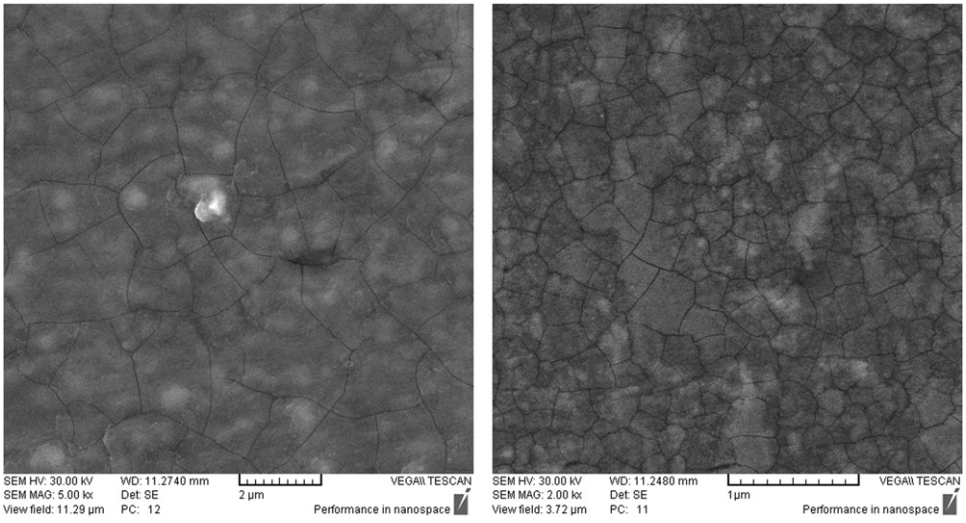

Fig. 3 Microstructure observations for initial and ECAPed Al after 8 passes by route A using SEM.

had been shown that the optimum superplastic ductility is achieved by route B_C because of the most expeditious generation of equiaxed grains with high angle grain boundaries (HAGBs). The results of Stolyarov et al. [17] indicated that route B_C is the most effective and route B_A is the least efficient in grain refinement. Also, routes B_A and C lead to elongated grains. Tong et al. [18] had surveyed the influence of ECAP routes on the microstructure and mechanical properties of Mg alloys. The results revealed that route B_C is the most capable in grain refinement and production of HAGBs, while route A is the least capable. In addition, Kim and Namkung [19] illustrated that routes A and B_A cause the lowest strain

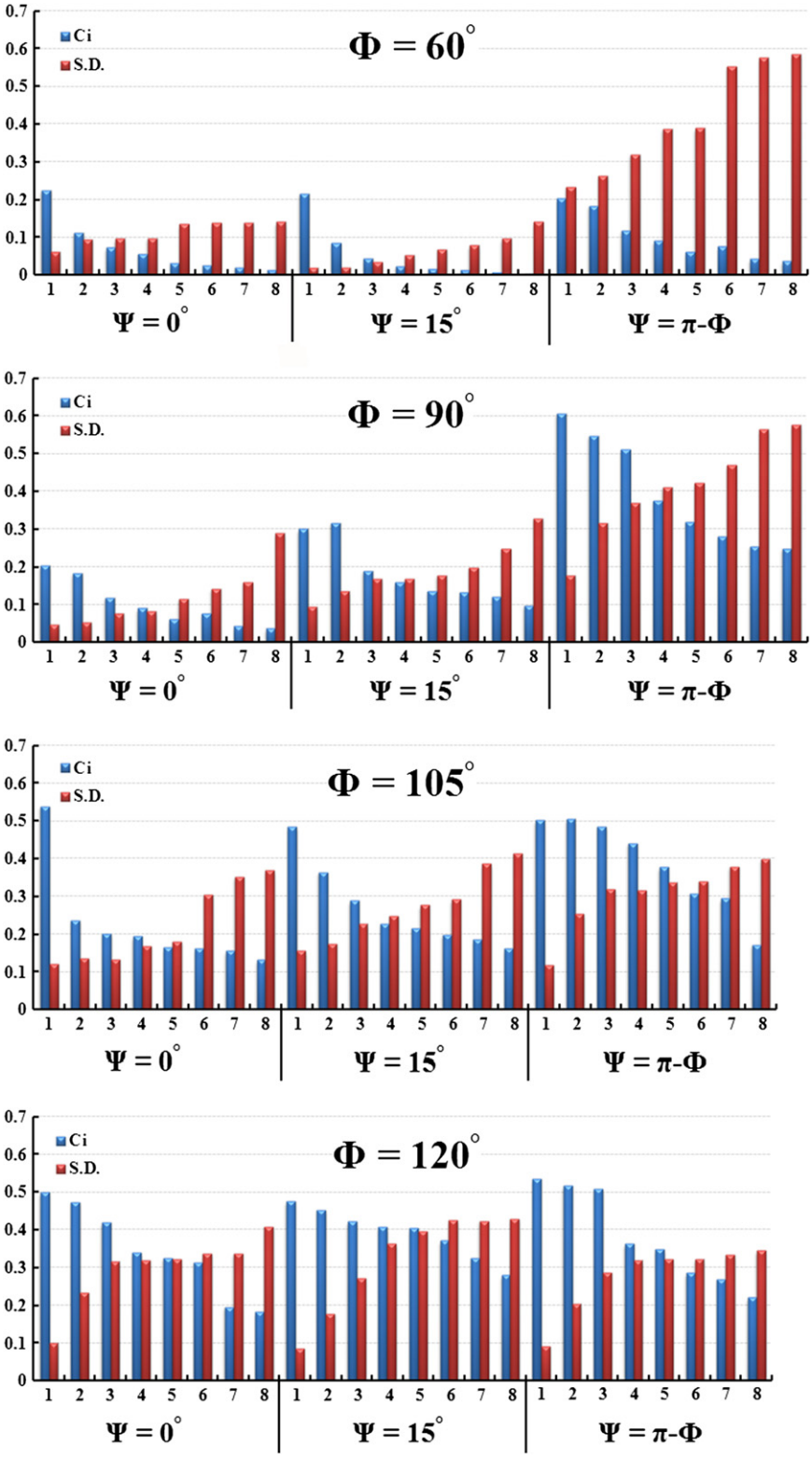

Fig. 4 The magnitudes of C_i and S.D. versus pass numbers in transverse direction.

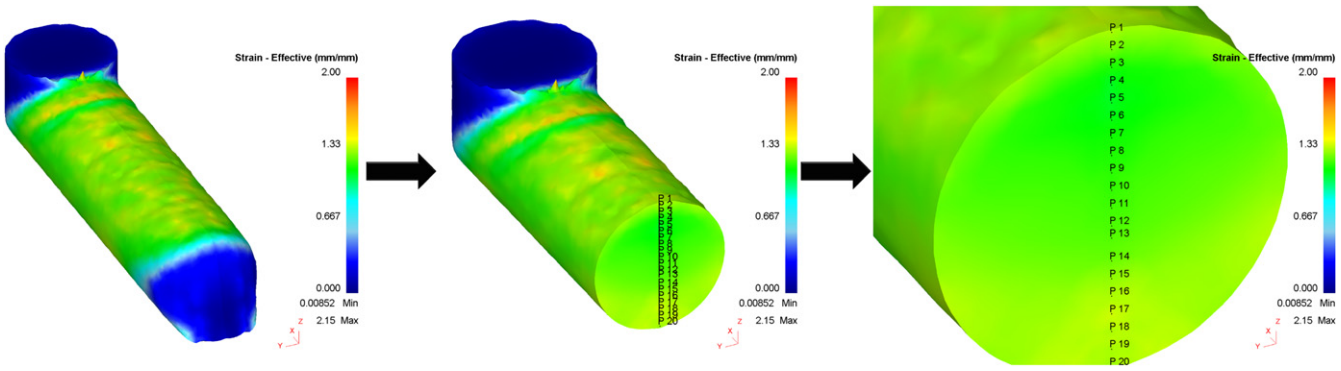

Fig. 5 Locations of 20 different nodes in the vertical centerline at the transverse direction of the work-piece.

distribution homogeneity and routes C and B_C give the highest strain dispersal uniformity.

On the other hand, several numerical researches have been performed to investigate the effects of different ECAP parameters including die channel angle, outer corner angle, friction coefficient, material properties, ram speed and temperature on the effective strain value, strain distribution uniformity, required pressing force value and material flow [20–23].

Although Eq. (2) represents the average effective strain magnitude induced to the specimen during each pass, different locations of the sample (in the transverse and longitudinal directions) experience different strain values depending on various parameters in the process. In general, there are two methods to quantify the degree of strain distribution homogeneity. One is inhomogeneity index (C_i) defined by Li et al. [24]:

$$C_i = \frac{\varepsilon_{max} - \varepsilon_{min}}{\varepsilon_{avg}} \tag{3}$$

where ε_{max}, ε_{min} and ε_{avg} denote the maximum, minimum and average of the plastic strain, respectively. A number of researchers have used inhomogeneity index (C_i) for investigating the strain distribution uniformity [24–29]. Less magnitude for C_i leads to better strain dispersal uniformity. According to Eq. (3), this factor depends only on the maximum, minimum and average magnitudes of plastic strain. The second method is a mathematical coefficient called standard deviation (S.D.) [30]. In addition, this parameter is utilized in statistical analyses in variant fields of sciences and humanities. In this study, S.D. has been employed to measure strain distribution uniformity expressed by

$$S.D. = \sqrt{\frac{\sum_{i=1}^{n} \left(\varepsilon_i - \varepsilon_{avg}\right)^2}{n}} \tag{4}$$

where ε_i is the plastic strain magnitude in ith node, ε_{avg} is the average value of plastic strain extracted from all nodes and n is the number of nodes in the billet. As is known, high value for S.D. indicates strain distribution non-uniformity.

Although a number of researches have been carried out on the efficiency of ECAP process routes and influences of various ECAP parameters on the strain behavior, there is no work up to now to design ECAP die based on the optimum strain behavior. In this paper, ECAP process strain distribution uniformity for different passes were compared using two factors inhomogeneity index (C_i) and standard deviation (S.D.). Furthermore, route A was used for examining these two strain distribution factors since this route gives the worst

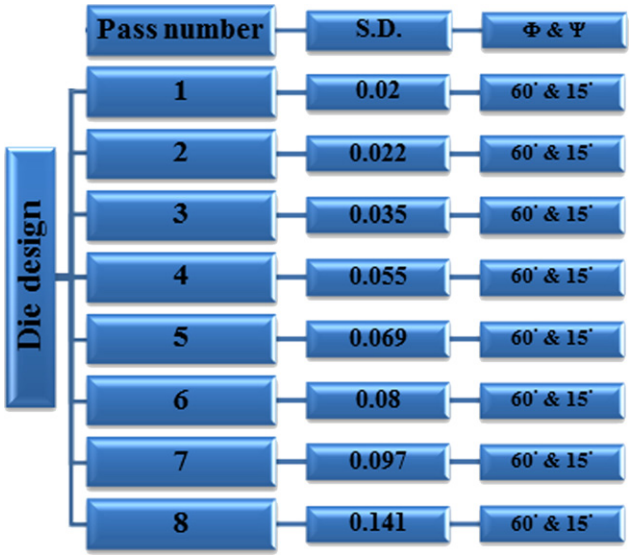

Fig. 6 ECAP die design based on strain distribution uniformity in transverse direction for 8 passes.

strain distribution homogeneity and the magnitude of strain heterogeneity increases by adding pass numbers. Also, ECAP process is experimentally performed on the commercial purity aluminum up to 8 passes by route A. The improvement of ECAPed Al properties has been demonstrated by accomplishing tensile test and microstructure observation. Influences of various die channel angles (60°, 90°, 105° and 120°) and outer corner angles (0°, 15° and $\pi - \Psi$) up to 8 passes on the strain behavior have been investigated numerically (96 different simulations). Finally, ECAP die design has been carried out based on the optimum strain distribution uniformity.

2. Experimental procedure

The material used in this study was commercial purity aluminum (chemical composition wt%: 99.5Al, 0.258Fe, 0.156Si, 0.0001Cu, 0.027Mg, 0.003Mn, 0.003V) annealed at 375 °C for 1 h and cooled slowly in furnace. Samples were prepared with diameter of 19.7 mm same as the ECAP die channel diameter and 180 mm length well lubricated in MoS_2 before pressing. An ECAP die with the channel angle of 90°, outer corner angle of 15° and channel diameter of 19.8 mm was designed and manufactured. The hydraulic press, ECAP die setup and billet after one pass

pressing are shown in Fig. 2. The ram speed was constant (equal to 2 mm/s) and ECAP process was performed at room temperature by route *A* up to 8 passes.

To prepare tensile test, specimens were machined with their longitudinal axes parallel to the pressing axis from the billet center according to ASTM B557M. To verify refining of the grain size during ECAP process, optical microscopy (OM) for initial billet and scanning electron microscopy (SEM) for ECAPed billet were applied to ensure the grain size reduction.

3. Finite element modeling

Simulations were carried out using commercial FEM software, DEFORM3D^{TM}. The work-piece was assumed to be plastic

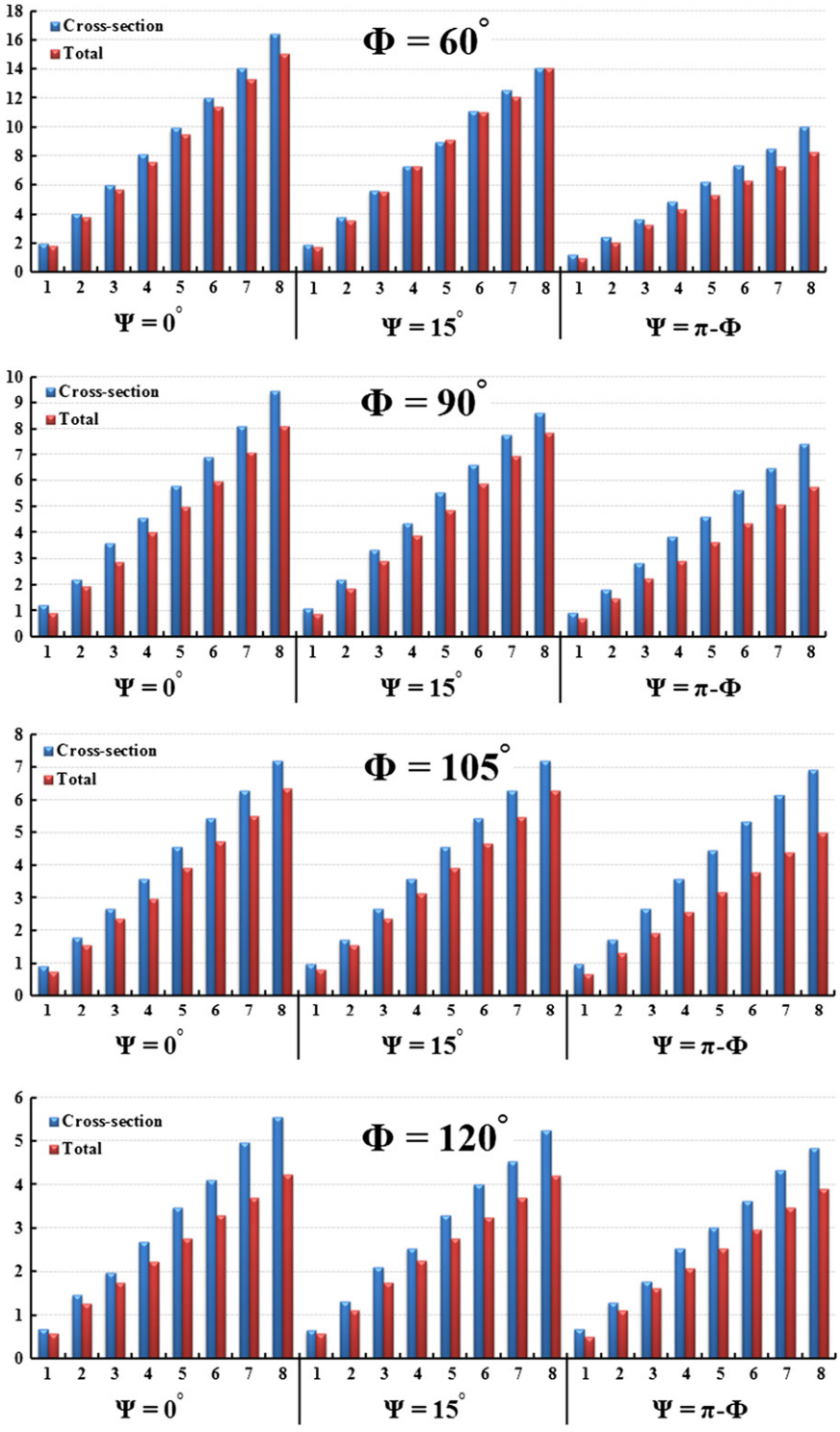

Fig. 7 The effective strain values for the 4 die channel angles and 3 outer corner angles up to 8 passes by route A.

having the same geometry with the experimental work. For the FEM analysis, the magnitudes of strain hardening coefficient (K=143 MPa) and strain hardening exponent (n=0.208) were obtained from true stress–true strain relationship in tensile test. The die and punch were supposed to be rigid. The value of 2 mm s^{-1} was assigned to the ram speed. In order to determine the optimum mesh size, mesh sensitivity diagram was plotted to investigate the convergence of results and selection of proper mesh element size. The optimum mesh element numbers were chosen as 10,000 and automatic re-meshing was used to accommodate large deformation in analyses. The value of 0.12 was selected as a friction coefficient [31] and all analyses were performed at the ambient temperature.

The pressing force is an important factor in metal forming and so, other significant parameters can affect this factor during the process. Hence as a validation of the FEM results, the required pressing force can be compared with the experimental work. If the punch force in the simulation meets well with that in the experiment at the same punch position with all similar conditions, the outputs in the FEM are considered as agreeable values.

After verification, various die channel angles (Φ=60°, 90°, 105° and 120°) and outer corner angles (Ψ=0°, 15° and $\pi-\Psi$) were simulated up to 8 passes via route A. Combination of these situations yields a total number of 96 runs. The effects of die channel angle, outer corner angle and pass number have been investigated on effective strain magnitude and strain distribution uniformity. Finally, the die design has been considered based on these parameters to achieve the optimum strain distribution homogeneity.

4. Results and discussion

4.1. Verification of FEM

To verify FEM work, the magnitude of pressing force has been measured in laboratory and compared with the FEM results. For one pass ECAP with commercial purity Al, the required pressing force magnitudes acquired from the experimental and the simulated works are 121.5 kN and 113 kN, respectively. This represents about 7% discrepancy between the experimental and numerical outcomes which is acceptable for all practical purposes.

4.2. Experimental results

Table 1 illustrates the magnitudes of yield strength (YS) and ultimate tensile strength (UTS) and also elongation to failure for commercial purity aluminum up to eight passes by route A. As can be seen, significant enhancements in the magnitudes of YS and UTS are obtained for the 1st pass and then, gradual increases are observed for subsequent passes. The same trend had been reported earlier [32,33]. YS and UTS values have been improved by 125%, 75% and 290%, 130% after 1st and 8th passes, respectively. The elongation to failure has been reduced by 45% and 65% after the 1st and 8th passes, respectively. This indicates that by increasing pass numbers, the ductility of aluminum tends to be dropped. Also, the average grain sizes measured before and after 8 pass ECAP are about 2 μm and 240 nm, respectively; see Fig. 3. As is known, the ECAP process consists of production, multiplication and locking of dislocations, making of low angle grain boundaries (LAGBs), HAGBs and finally, formation of UFG materials [32–34].

4.3. Numerical results

4.3.1. Strain distribution uniformity parameters

Two parameters (inhomogeneity index (C_i) and standard deviation (S.D.)) have been applied to measure and investigate strain distribution homogeneity. Increasing pass number by route A results in decrease of strain distribution uniformity [19]. So, it is anticipated that C_i and S.D. values would increase by increasing pass number. The magnitudes of inhomogeneity index and standard deviation are presented in Fig. 4 for all 96 ECAP circumstances. These conditions are the combinations of 4 die channel angles (Φ=60°, 90°, 105° and 120°) and 3 outer corner angles (Ψ=0°, 15° and $\pi-\Psi$) up to 8 passes by route A. These values have been calculated from the 20 effective strain magnitudes at the cross-sectional area in the mid-length of the billet as shown in Fig. 5.

As can be observed in Fig. 4, the inhomogeneity index is reduced with increasing pass number. It means that ECAPed aluminum with uniform strain distribution is obtained by increasing pass number. This is inconsistent with the previous experimental and numerical investigations where the pass number increase by route A leads to non-uniformity in the strain dispersal [19]. Also, it has been demonstrated that the volume of fully worked material is continuously reduced by increasing the number of passes and as a result, ECAPed material with a strong texture or anisotropic grain morphology is obtained by this route [35]. So, for route A ECAPed materials, the degree of strain inhomogeneity cannot be quantified with C_i factor. On the other hand, S.D. value indicates that strain distribution heterogeneity is increasing as the number of passes increases. It can thus be said that at least for route A, the S.D. is a better indication of quantifying the strain distribution homogeneity of ECAPed materials than C_i.

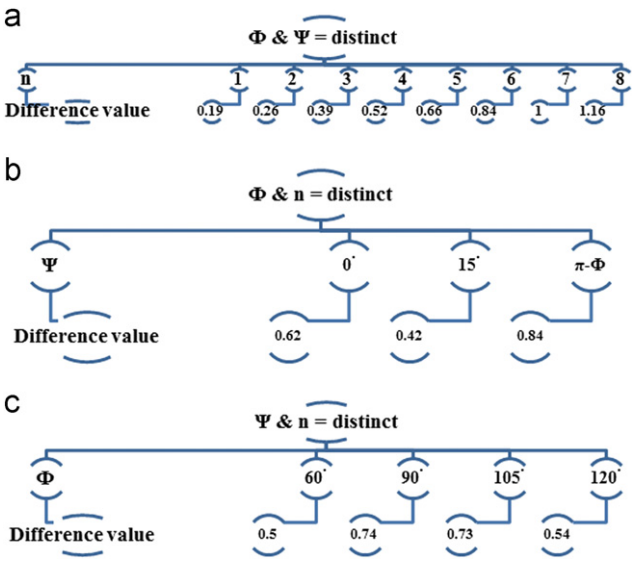

Fig. 8 The magnitudes of effective strain differences between the cross-section and whole of the work-piece.

4.3.2. Die design based on the strain distribution homogeneity in the transverse direction

The optimum combinations of Φ and Ψ to achieve minimum S.D. value in the transverse direction for 8 passes are listed in Fig. 6.

As can be seen, the best strain dispersal homogeneity can be obtained with $\Phi=60^\circ$ and $\Psi=15^\circ$. In addition, the die channel angle of 60° leads to a higher magnitude of effective strain than the other 3.

4.3.3. Die design based on the strain distribution homogeneity in the sample

Up to now, most of the ECAP die design has been based on the effective strain magnitude. Achieving a certain amount of grain refinement or effective strain value can be obtained with increasing pass number, but, the authors believe that the most prominent factor in this process is the strain distribution uniformity which leads to homogenous ECAPed materials. Fig. 7 represents the effective strain magnitude for the 4 die channel angles and 3 outer corner angles up to 8 passes by route *A* at the cross-section and in the bulk of the samples. The position of the cross-section is indicated in Fig. 5.

As a first result, the effective strain value at the cross-section is higher or at least equal to that of the entire billet. It may be related to the undeformed regions of the ECAPed material in the head and tail parts of the sample. The existence of these sections reduces the effective strain magnitude in the whole of the sample. The minimum and maximum differences between the effective strain at the cross-section and entirety of

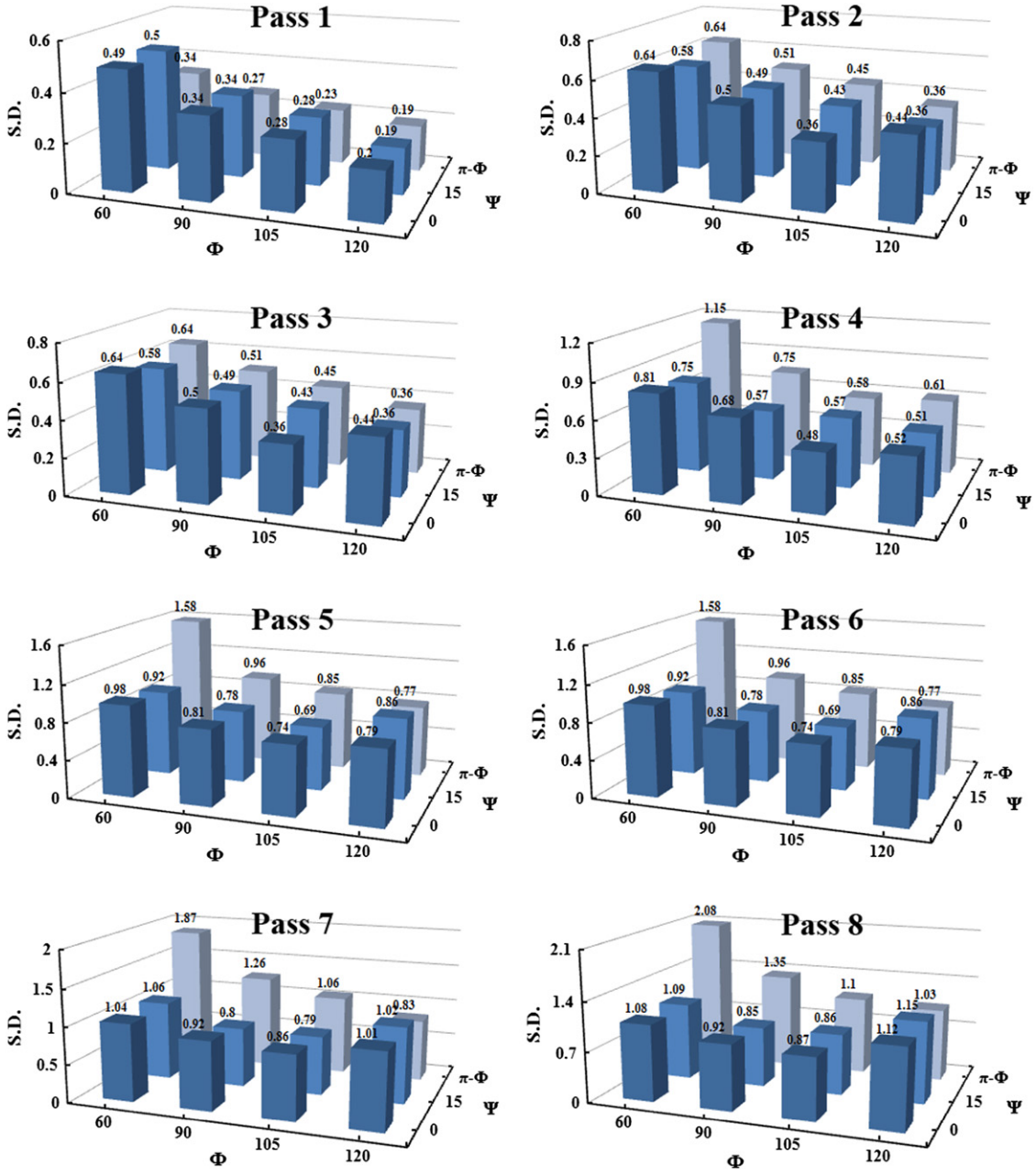

Fig. 9 The S.D. magnitudes for the different values of die channel and outer corner angles from 1 to 8 passes.

the billet are 0.01 and 1.93 referred to the cases of $\Phi=60^\circ$, $\Psi=15^\circ$ and 4th pass and $\Phi=105^\circ$, $\Psi=75^\circ$ and 8th pass, respectively. Also, the dissimilarity value between the effective strain at the cross-section and whole of the sample intensifies by increasing pass number irrespective of the die parameters (Φ and Ψ), as exhibited in Fig. 8a. These values are averaged magnitudes calculated from the effective strain differences at the cross-section and whole of the sample for the 4 die channel angles and 3 outer corner angles. The average difference between the effective strain at the cross-section and entity of the billet for the 4 die channel angle and 8 passes versus outer corner angles is represented in Fig. 8b. It is observed that less disparity is obtained when the outer corner angle is equal to 15°. Finally for different die channel angles, the magnitude of effective strain differences at the cross-section and whole of sample is expressed in Fig. 8c. In this circumstance, the differences are averaged for the 3 outer corner angles and 8 passes. As a conclusion of this figure, 1st pass, $\Psi=15^\circ$ and $\Phi=60^\circ$ gives the least effective strain differences between the cross-section and whole of the ECAPed Al.

Fig. 9 shows the S.D. values for different die channel angles, outer corner angles and pass numbers.

Firstly, the magnitude of S.D. increases with increasing pass numbers for every die channel and outer corner angles. This means that increasing pass number results in a lower strain distribution uniformity in materials. The average magnitudes of S.D. are listed in Fig. 10 for each pass number (up to 8 passes) calculated from the 4 die channel angles and 3 outer corner angles.

Secondly as mentioned earlier, we believe that the die which produces more isotropic ECAP material is more suitable and important than the one which produces higher effective strain value. For this consideration, the suitable combination of Φ and Ψ are ($\Phi=120^\circ$ and $\Psi=15^\circ$) and ($\Phi=120^\circ$ and $\Psi=60^\circ$), together. It is noted that for the die channel angle of 120°, the magnitude of S.D. is virtually independent on the outer corner angle. Finally for ECAPing of Al, the optimum parameters for die design depend on the pass number as listed in Table 2.

As indicated in Table 2, the optimum values of die design parameters are $\Phi=120^\circ$ and $\Psi=15^\circ$ or 60°. Although material in these die design conditions gives better strain distribution homogeneity, the effective strain magnitude is not the highest. However, increasing pass numbers can produce the desire amount of effective strain.

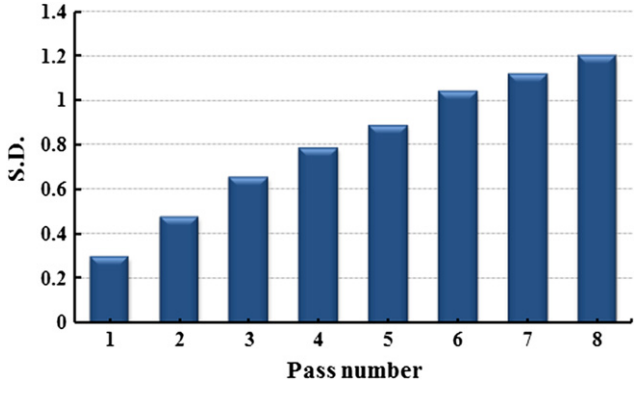

Fig. 10 The average S.D. values for each pass number up to 8 passes irrespective of die channel and outer corner angles.

Table 2 The magnitudes of die design parameters to achieve the optimum strain distribution uniformity in the ECAPed sample.

No. of passes	S.D.	ECAP die design parameters	
		Φ	Ψ
1	0.19	120	15 and $\pi-\Psi$
2	0.36	120	15 and $\pi-\Psi$
3	0.48	105	0
4	0.61	105	0
5	0.69	105	15
6	0.79	105	15
7	0.85	90	15
8	0.87	105	15

5. Conclusion

In the current study, combinations of 4 die channel angles ($\Phi=60^\circ$, 90°, 105° and 120°), 3 outer corner angles ($\Psi=0^\circ$, 15° and $\pi-\Psi$) and pass numbers (up to 8 passes) have been simulated by route *A*. The influences of above factors on the effective strain magnitude and strain distribution behavior via two parameters (inhomogeneity index and standard deviation) at the transverse direction and whole of the samples are investigated. The prominent conclusions can be drawn as follows:

- For route *A* ECAP, the magnitude of S.D. increases with increasing pass number; i.e. less strain distribution homogeneity is achieved using route *A* by increasing pass numbers.
- Considering that the increasing pass number causes high strain distribution heterogeneity, inhomogeneity index (C_i) is not a suitable candidate to quantify the strain dispersal homogeneity. On the other hand, standard deviation (S.D.) is a better factor for quantifying the strain distribution uniformity of ECAPed materials.
- 1st pass, $\Psi=15^\circ$ and $\Phi=60^\circ$ are the general guidelines to obtain the least effective strain differences between the transverse plane and whole of the ECAPed Al.
- $\Phi=60^\circ$ and $\Psi=15^\circ$ are the values of optimum parameters to design ECAP die based on the best strain distribution uniformity at the cross-section of the sample.
- $\Phi=120^\circ$ and $\Psi=15^\circ$ or 60° are the magnitudes of die channel angle and outer corner angle for designing ECAP die to achieve optimum strain dispensation homogeneity at the bulk of the work-piece.

In the experimental work, pure Al was subjected to ECAP die with the channel angle of 90° and outer corner angle of 15° up to 8 passes by route *A*. Improvement of the ECAPed aluminum properties was confirmed with increasing YS and UTS (about 4 and 2 times, respectively) and also, reduction of the grain size (about 8 times).

Acknowledgment

The authors wish to thank Mr. H. Nomoradi for providing the SEM micrographs used in this work.

References

[1] V.M. Segal, Equal channel angular extrusion: from macromechanics to structure formation, Materials Science and Engineering A 271 (1999) 322–333.

[2] S.L. Semiatin, D.P. DeLo, Equal channel angular extrusion of difficult-to-work alloys, Materials and Design 21 (2000) 311–322.

[3] L. Kommel, I. Hussainova, O. Volobueva, Microstructure and properties development of copper during severe plastic deformation, Materials and Design 28 (2007) 2121–2128.

[4] Ruslan Z. Valiev, Terence G. Langdon, Principles of equal-channel angular pressing as a processing tool for grain refinement, Progress in Materials Science 51 (2006) 881–981.

[5] Minoru Furukawa, Yoshinori Iwahashi, Zenji Horita, Minoru Nemoto, Terence G. Langdon, The shearing characteristics associated with equal-channel angular pressing, Materials Science and Engineering A 257 (1998) 328–332.

[6] Alexander P. Zhilyaev, Terence G. Langdon, Using high-pressure torsion for metal processing: fundamentals and applications, Progress in Materials Science 53 (2008) 893–979.

[7] Y. Saito, N. Tsuji, H. Utsunomiya, T. Sakai, R.G. Hong, Ultra-fine grained bulk aluminum produced by accumulative roll-bonding (ARB) process, Scripta Materialia 39 (9) (1998) 1221–1227.

[8] Dong Hyuk Shin, Jong-Jin Park, Yong-Seog Kim, Kyung-Tae Park, Constrained groove pressing and its application to grain refinement of aluminum, Materials Science and Engineering A 328 (2002) 98–103.

[9] S.M. Fatemi-Varzaneh, A. Zarei-Hanzaki, Accumulative back extrusion (ABE) processing as a novel bulk deformation method, Materials Science and Engineering A 504 (2009) 104–106.

[10] Ghader Faraji, Mahmoud Mosavi Mashhadi, Hyoung Seop Kim, Tubular channel angular pressing (TCAP) as a novel severe plastic deformation method for cylindrical tubes, Materials Letters 65 (2011) 3009–3012.

[11] I. Balasundar, M.Sudhakara Rao, T. Raghu, Equal channel angular pressing die to extrude a variety of materials, Materials and Design 30 (2009) 1050–1059.

[12] Terence G. Langdon, The principles of grain refinement in equal-channel angular pressing, Materials Science and Engineering A 462 (2007) 3–11.

[13] F. Djavanroodi, M. Ebrahimi, B. Rajabifar, S. Akramizadeh, Fatigue design factors for ECAPed materials, Materials Science and Engineering A 528 (2010) 745–750.

[14] Cheng Xu, Minoru Furukawa, Zenji Horita, Terence G. Langdon, Severe plastic deformation as a processing tool for developing superplastic metals, Journal of Alloys and Compounds 378 (2004) 27–34.

[15] Irene J. Beyerlein, László S. Tóth, Texture evolution in equal-channel angular extrusion, Progress in Materials Science 54 (2009) 427–510.

[16] Shogo Komura, Minoru Furukawa, Zenji Horita, Minoru Nemoto, Terence G. Langdon, Optimizing the procedure of equal-channel angular pressing for maximum superplasticity, Materials Science and Engineering A 297 (2001) 111–118.

[17] Vladimir V. Stolyarov, Y.Theodore Zhu, Igor V. Alexandrov, Terry C. Lowe, Ruslan Z. Valiev, Influence of ECAP routes on the microstructure and properties of pure Ti, Materials Science and Engineering A 299 (2001) 59–67.

[18] L.B. Tong, M.Y. Zheng, X.S. Hu, K. Wu, S.W. Xu, S. Kamado, Y. Kojima, Influence of ECAP routes on microstructure and mechanical properties of Mg–Zn–Ca alloy, Materials Science and Engineering A 527 (2010) 4250–4256.

[19] W.J. Kim, J.C. Namkung, Computational analysis of effect of route on strain uniformity in equal channel angular extrusion, Materials Science and Engineering A 412 (2005) 287–297.

[20] Z.J. Zhang, I.H. Son, Y.T. Im, J.K. Park, Finite element analysis of plastic deformation of CP-Ti by multi-pass equal channel angular extrusion at medium hot-working temperature, Materials Science and Engineering A 447 (2007) 134–141.

[21] Roberto Braga Figueiredo, Maria Teresa Paulino Aguilar, Paulo Roberto Cetlin, Finite element modelling of plastic instability during ECAP processing of flow-softening materials, Materials Science and Engineering A 430 (2006) 179–184.

[22] F. Djavanroodi, M. Ebrahimi, Effect of die parameters and material properties in ECAP with parallel channels, Materials Science and Engineering A 527 (2010) 7593–7599.

[23] P. Karpuz, C. Simsir, C. Hakan Gür, Investigating the effects of hardening of aluminium alloys on equal-channel angular pressing—a finite-element study, Materials Science and Engineering A 503 (2009) 148–151.

[24] S. Li, M.A.M. Bourke, I.J. Beyerlein, D.J. Alexander, B. Clausen, Finite element analysis of the plastic deformation zone and working load in equal channel angular extrusion, Materials Science and Engineering A 382 (2004) 217–236.

[25] Tao Suo, Yulong Li, Yazhou Guo, Yuanyong Liu, The simulation of deformation distribution during ECAP using 3D finite element method, Materials Science and Engineering A 432 (2006) 269–274.

[26] Tao Suo, Yulong Li, Qiong Deng, Yuanyong Liu, Optimal pressing route for continued equal channel angular pressing by finite element analysis, Materials Science and Engineering A 466 (2007) 166–171.

[27] V. Patil Basavaraj, Uday Chakkingal, T.S. Prasanna Kumar, Study of channel angle influence on material flow and strain inhomogeneity in equal channel angular pressing using 3D finite element simulation, Journal of Materials Processing Technology 209 (2009) 89–95.

[28] Hong-jun Hu, Ding-fei Zhang, Fu-sheng Pan, Die structure optimization of equal channel angular extrusion for AZ31 magnesium alloy based on finite element method, Transactions of the Nonferrous Metals Society of China 20 (2010) 259–266.

[29] Nahed El Mahallawy, Farouk A. Shehata, Mohamed Abd El Hameed, Mohamed Ibrahim Abd El Aal, Hyoung Seop Kim, 3D FEM simulations for the homogeneity of plastic deformation in Al–Cu alloys during ECAP, Materials Science and Engineering A 527 (2010) 1404–1410.

[30] F. Zaïri, B. Aour, J.M. Gloaguen, M. Naït-Abdelaziz, J.M. Lefebvre, Numerical modelling of elastic–viscoplastic equal channel angular extrusion process of a polymer, Computational Materials Science 38 (2006) 202–216.

[31] F. Djavanroodi, M. Ebrahimi, Effect of die channel angle, friction and back pressure in the equal channel angular pressing using 3D finite element simulation, Materials Science and Engineering A 527 (2010) 1230–1235.

[32] M. Reihanian, R. Ebrahimi, N. Tsuji, M.M. Moshksar, Analysis of the mechanical properties and deformation behavior of nanostructured commercially pure Al processed by equal channel angular pressing (ECAP), Materials Science and Engineering A 473 (2008) 189–194.

[33] K.J. Kim, D.Y. Yang, J.W. Yoon, Microstructural evolution and its effect on mechanical properties of commercially pure aluminum deformed by ECAE (Equal Channel Angular Extrusion) via routes A and C, Materials Science and Engineering A 527 (2010) 7927–7930.

[34] Zubear Ahmed Khan, Uday Chakkingal, P. Venugopal, Analysis of forming loads, microstructure development and mechanical property evolution during equal channel angular extrusion of a commercial grade aluminum, Journal of Materials Processing Technology 135 (2003) 59–67.

[35] R.E. Barber, T. Dudo, P.B. Yasskin, K.T. Hartwig, Product yield for ECAE processing, Scripta Materialia 51 (2004) 373–377.